

# In-silico Modulation of the Irinotecan Release from a Functionalized MCM-41 Support

I. Luta and G. Maria\*

Department of Chemical Engineering,  
University Politehnica of Bucharest, Romania

Original scientific paper  
Received: April 16, 2012  
Accepted: August 31, 2012

The release rate of a drug molecule from a porous support depends on a large number of factors, including support characteristics, surface functionalization (procedure and linker type), drug features, biological receptor fluid characteristics, and release conditions. Model-based (*in-silico*) modulation of the release rate through influential parameters can help in designing an optimized delivery system for a specific drug action. To prevent biased predictions, a dynamic mechanism-based model was adopted, by including kinetic terms related to surface adsorption-desorption, diffusion in pores, and external diffusion of the drug to the body fluid. Exemplification is made for the case of a functionalized silica MCM-41 support with a tunable pore size distribution and functionalization possibilities with hydrophobic (triethoxyvinylsilane, VTES) or hydrophilic (3-aminopropyl triethoxysilane, APTES) linkers. Variation of several structural parameters, referring to the average pore size, initial drug load, and linker proportion on a bi-functionalized support, pointed out the strong nonlinear relationships between the process variables and the release rate.

*Key words:*

Drug delivery; *in-silico* design; irinotecan release; MCM-41; bi-functionalization; kinetic modelling

## Introduction

Over the last decades, extensive experimental efforts have been made for studying and designing optimized drug delivery systems, using both natural and artificial materials as drug carriers. Porous (silica, alumino-silica, polymers, gels, carbon based), amorphous colloidal, or hybrid inorganic-organic supports open a wide range of options to develop an efficient release system.<sup>1</sup> Surfaces modified by (multi-)functionalization are used to control the release of drugs, proteins, and other bioactive compounds into body fluids (gastric, intestinal, or plasma) with a wide range of applications in medicine and industrial area.<sup>2–5</sup> Various alternatives of drug(ligand)-linker-support systems have been investigated, trying to “program” the drug release into a target environment.

Currently, optimized drug delivery systems can be designed for every specific molecule and desired action.<sup>2</sup> In the pre-programmed drug delivery, the release rate is adjusted by the system characteristics controlling the diffusion in the polymeric/inorganic matrix, across the support membrane, or from a micro-reservoir containing a homogeneous dispersion / heterogeneous suspension of drug particles in a lipophilic/hydrophilic polymeric matrix / solution.

In the activated drug delivery systems, the release rate is induced and controlled by physical (osmotic or hydrodynamic pressure, mechanical, magnetic, ultrasonic forces), chemical (pH, ionic strength, redox agents), or biochemical (enzymes) means. In the feedback-regulated release, various triggering agents, present in the body fluid, activate and control the drug release rate by a slow erosion of the functionalised membrane, by controlling the membrane permeability, or simply by chemical reaction with the support-ligand system.<sup>6</sup> Modern technologies of developing molecularly imprinted supports (MIP, with covalently or non-covalently coupled drug) are currently used for designing intelligent drug release systems, feedback controlled or site targeting, triggered by a specific agent or by MIP binding to a specific tissue.<sup>7</sup> Such a highly controlled release is the result of designing systems with molecular recognition properties, and of applying specific preparative strategies that place binding or functional groups at defined positions in imprinted sites of the support.<sup>8</sup>

Among carriers, ordered mesoporous supports proved to be very suitable for designing a controlled release system, due to excellent adsorption properties, a high specific surface area and porosity, high stability, tunable pore size with narrow distribution, biocompatibility, easy functionalization allowing to modulate the release rate.<sup>5,9,10</sup> Functionalization of

\*Corresponding author; Mail address: P.O. 35–107 Bucharest, Romania;  
Email: gmaria99m@hotmail.com

the support with suitable crosslinkers allows incorporating organic / hybrid species in the porous support for bonding guest molecules, thus changing dramatically the support surface properties (hydrophilicity, hydrophobicity, resistance to surface attack agents).<sup>1</sup> Grafting the support surface with passive or active groups, surface coating, or the use of co-condensation reactions are the most common methods for surface functionalization via covalent bonding of organic groups. In the post-synthesis method, grafting the silanol groups with hydrophobic alkyl or phenyl groups, or with hydrophilic aminopropyl or mercaptopropyl groups, is a very flexible technique to tailor the pore and particle size, as well as the surface polarity. The direct synthesis (“one-pot” reaction) involves co-condensation of tetraalkoxysilane with organoalkoxysilanes in the presence of a surfactant leading to hybrid inorganic-organic matrices with a more homogeneous surface coverage but with the disadvantage of breaking the matrix integrity for high coverage percentages.<sup>1,11</sup> Multi-functional surfaces can also be obtained, although the location of different functional groups cannot be as much controlled as by grafting process.

One particular class of silica supports are the mesoporous MCM and SBA, intensively used as carrier matrix for a large number of drugs, such as antibiotics of different generations (e.g. gentamicin, erythromycin, tetracycline, etc.), anti-inflammatory drugs (aspirin, ibuprofen, diflunisal, naproxen), anti-cancer drugs (e.g. irinotecan, cisplatin, taxotere, taxol, navcelbine, methotrexate), vitamins, etc.<sup>5,9,12,13</sup> The advantage of these supports is coming from the very ordered structure including regular and straight pores (e.g. hexagonal array with pore sizes of 20–50 Å for MCM-41), a high porosity (0.6–0.8), high BET surface area (500–1260 m<sup>2</sup> g<sup>-1</sup>), and a high drug uptake capacity.<sup>11,13–16</sup> Being covered with siloxane bridges and free silanol groups, the surface availability for a certain drug can be adjusted by functionalization with hydrophobic / hydrophilic silylating agents or reactive groups (e.g. nitriles, alkylthiols, alkyl amines, alkylsilane linkers).<sup>1,10,11,17</sup> The release rate can also be changed by pore size modulation using various surfactants,<sup>14,18</sup> by increasing the adsorption capacity with varying the Si/Al ratio in hybrid supports,<sup>19</sup> or by eventually coating the support with a suitable membrane.<sup>1,12</sup>

To design an optimized delivery system for a specified drug, steady experimental investigations try to separate the contribution of influential factors: support structural properties (composition, morphology, specific surface area, porosity / pore volume, tortuosity, pore sizes and their distribution), drug features (structure, solubility, stability, uptake on the support, diffusivity), linker charac-

teristics (structure, hydrophilicity / hydrophobicity, amount), biological fluid interacting with the drug-linker-support system (composition, redox / ionic activity, presence of activating agents), release conditions (pH, temperature, stirring).<sup>2,6,10,13,20,21</sup> Laboratory experiments in a synthetic medium are usually employed, even if they cannot reproduce the whole system complexity, thus leading to limited interpretations.

To better correlate the results, various kinetic and thermodynamic models have been proposed, of complexity depending on the available information and utilization scope. Based on these, *in-silico* design of an optimized delivery system can be developed leading to: i) a considerable reduction in the experimental effort by using the predictive capacity of an adequate and robust model; ii) possibility to highlight the physico-chemical-biological influential factors and their individual action mode on the release rate and equilibrium state; iii) possibility to correlate the system characteristics with the model parameters; iv) possibility to direct the experimental effort toward the most favourable delivery configuration for a specified drug and action type. Even if experimental checks of the model predictions remain an essential issue, the *in-silico* activities can considerably reduce the design effort.

For a precise prediction of the process dynamics [that is the time dependent mass of released drug until a certain time  $M(t)$ ], an adequate mathematical model has to be employed. The use of simple empirical models for the diffusion in support or membrane, for swelling systems, or for a chemically controlled release (e.g. power-law model  $M(t)/M_{\infty} = kt^n$  of  $n$ -th order, growing exponential, or models of zero-, first-, or second-order apparent rate; review of Maria & Luta<sup>6</sup>) usually present inconsistent parameters, dependent on the initial drug load, and requiring additional statistical correlations with the structural characteristics of the drug-support system.<sup>2,3,5,14,21–24</sup> Alternatively, a mechanistic based dynamic model, including terms related to the physico-chemical adsorption-desorption on the surface, internal and external diffusion steps, and structural/operating parameters can offer more precise, robust and interpretable predictions. The model should be able to predict, under sink or non-sink conditions, the variation of drug concentration in the bulk phase, with rate constants independent of the initial drug dose or fluid concentrations. For instance, various diffusion models have been elaborated in one or several phases (support matrix, pores, coating membrane, external liquid), by using Fick-type equations solved for different geometries (thin sheet, rectangular parallelepiped, cylinder of finite or infinite length, sphere), with known initial (uniform or non-uniform field distri-

bution in the solid) and boundary conditions (at the solid-liquid or membrane interface with an external diffusion layer or with bulk liquid).<sup>2,6,13,22,25</sup> By including parameters that quantify the system structure and environment characteristics, such models are suitable to *in-silico* modulate the system properties for obtaining a desired drug release.

Recently, Maria et al.<sup>13,26</sup> proposed a compartmented mechanistic model (denoted here as “Extended Kinetic Model” – EKM), by including a minimum number of terms describing the surface physico-chemical interactions between drug and (un)functionalized surface, the Fickian diffusion in pores and in the external liquid film. The model was proved to adequately represent the release of various biological active molecules, such as irinotecan (but also some cephalosporines, anti-TBC, and other drugs) from mesoporous silica carriers, with the advantage of including consistent and interpretable parameters, independent on the initial drug load. The EKM includes parameters related to the support morphology (specific surface area, porosity, pore volume, tortuosity, average pore size), and rate constants related to the support-linker chemical structure, functionalization type, and operating conditions.

The aim of this paper is to check the possibility of using the EKM to *in-silico* modulate the drug release rate by varying structural and operating conditions, leading to design a drug delivery system with a controlled release. Exemplification is made for a silica MCM-41 support, functionalized with hydrophobic triethoxyvinylsilane (VTES) or hydrophilic 3-aminopropyl triethoxysilane (APTES) linkers, and used for the release of irinotecan into a synthetic intestinal fluid. The study will be focus on modulating the internal resistance parameters that is the average pore size, initial drug load and linker proportion on a bi-functionalized support. The model is applied to spherical support particles, but other configurations (e.g. porous cylindrical tablets, or thin films) can be easily approached by evaluating the particle effectiveness and mass transfer coefficients with recommended relationships from literature.<sup>27,28</sup>

## Drug adsorption-desorption model

The adopted EKM for describing the drug adsorption-desorption on porous solid supports (without membrane or swelling properties)<sup>13,26</sup> considers three drug “forms”, belonging to three homogeneous phases in contact: the “free” drug ( $A_f^s$ ) moving in the liquid filling the pores; the “bonded” drug ( $A_b^s$ ) absorbed on the solid matrix sites (directly or via a linker molecule L); the “external”

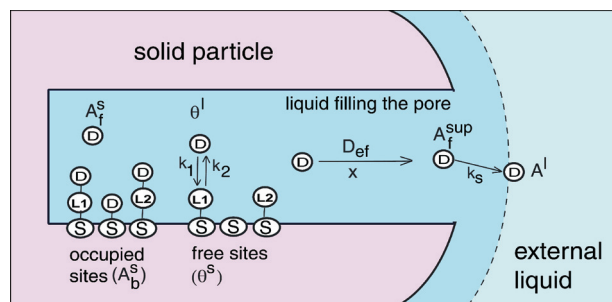


Fig. 1 – The hypothetical mechanism of drug (D) adsorption-desorption on functionalized surface sites (S) with linkers (L1,L2) and the drug diffusion in the porous solid support (adapted from Maria et al.<sup>13</sup>)

drug ( $A^l$ ) dissolved in the external liquid / bulk convective phase (see schema of Figure 1; A denotes the concentration of the drug species referred here to the liquid volume, but solid volume or mass can be used as well). Drug adsorption-desorption occurs until the equilibrium among phases is reached. For a soluble drug in the receptor liquid, the EKM includes the following terms (Table 1, see also the Appendix of Maria et al.<sup>26</sup>):

i) adsorption-desorption reactions on the surface, of bimolecular type in both directions,  $A_b^s + \theta^l \xrightleftharpoons[k_1]{k_2} A_f^s + \theta^s$ , the triggering forces being the drug adsorption potential (proportional to the free site concentration,  $\theta^s = A_b^{s, \max} - A_b^s$ ), and the drug desorption potential (proportional to the fluid unsaturation degree,  $\theta^l = A_f^{\max} - A_f^s$ ). The model assumes that adsorption sites are uniformly distributed on the homogeneous surface, being equally accessible to the drug molecules, the drug being disposed in a mono-molecular layer on the active sites (adsorption on the pore walls is neglected,  $K_p = 1$ ).

ii) diffusional flow rate of the drug through the pore cross-section at interface ( $J_{diff,s}$ ), the transport resistance in the particle being synthetically expressed by the effectiveness factor ( $\eta$ ). Particle effectiveness is evaluated by means of Thiele modulus ( $\phi$ ), which is dependent on the particle diameter ( $d_p$ ), rate constants ( $k_1, k_2$ ), and the effective diffusivity in pores ( $D_{A,ef}$ , see its evaluation in Table 1; Knudsen and surface diffusion are neglected, the former being of three orders of magnitude higher than the molecular diffusivity). According to this method, the drug concentration at the solid surface ( $A_f^{sup}$ ) is considered only function of time, its values resulting from solving the steady-state equality of fluxes through the solid surface and the external liquid film.

iii) diffusion flux of the drug in the external liquid film surrounding the support particle to/from the receptor body fluid (considered homogeneous) due to the concentration gradients. Evaluation of

Table 1 – Extended kinetic model (EKM) describing the drug adsorption-desorption and diffusional transport through the porous support (see notations of Fig. 1; after Maria et al.<sup>13,26</sup>)

Model terms	Parameters / conditions
Surface reaction: $A_b^s + \theta^l \xrightleftharpoons[k_1]{k_2[AA]} A_f^s + \theta^s$	Adsorption / desorption potential: $\theta^s = A_b^{s,max} - A_b^s; \text{ (free sites)}$ $\theta^l = A_f^{max} - A_f^s; \text{ (unsaturated liquid)}$
Mass balance equations: $\frac{dA_b^s}{dt} = k_1 A_f^s \theta^s - k_2 A_b^s \theta^l$ $\frac{dA_f^s}{dt} = -k_1 A_f^s \theta^s + k_2 A_b^s \theta^l - J_{diff,s}$ $\frac{dA^l}{dt} = J_{diff,s}$	Initial conditions ( $t = 0$ ): $A_b^s = A_b^{s,0}; A_f^s = A_f^{s,0}; A^l = A^l_0;$ Apparent desorption rate constant: $k_2 = k_2[AA]; \text{ AA = desorption activators from the receptor liquid;}$ Equilibrium constant on surface: $K = k_2/k_1$
Evaluation of $A_f^{sup}$ (quasi-steady-state diffusion at the solid interface; $A_f^s$ is replaced by $A_f^{sup}$ ):	
$r_A^{sup} = \eta(k_1 A_f^{sup} \theta^s - k_2 A_b^s \theta^{l, sup}) = J_{diff,s} = k_s a_s (A_f^{sup} - A^l)$	
Spherical particle effectiveness factor: <sup>22,35,36</sup> $\eta = (3\phi \coth(3\phi) - 1)/(3\phi^2)$ $\phi = (d_p/6)\sqrt{(k_1 \theta^s + k_2 \theta^l)/D_{A,ef}}$	$D_{A,ef} \approx D_A K_p K_r \varepsilon_p / \tau_p; \quad K_p \approx 1;$ $K_r = (1 - d_{A,i}/d_{pore})^2;$ $\tau_p^2 = \frac{\varepsilon_p}{1 - \sqrt[3]{1 - \varepsilon_p}}; \quad \varepsilon_p = V_{TP} \rho_p$
External mass transfer resistance: <sup>28,31,34</sup> $k_s = Sh \times D_A / d_p; \quad a_s = (6\varepsilon_s)/d_p$ $Sh = (2 + 0.4 Re_{lq}^{0.25} Sc_{lq}^{0.33}) \varphi_C$ $Re_{lq} = \sum_{lq} d_p^4 \rho_{lq}^3 / \mu_{lq}^3; \quad Sc_{lq} = \mu_{lq} / (\rho_{lq} D_A)$	$\sum_{lq} = g u_{s,lq} (\rho_s \varepsilon_s + \rho_{lq} \varepsilon_{lq}) / (\rho_s \varepsilon_s)$ $\varepsilon_{lq} = 1 - \varepsilon_s; \quad u_{s,lq} = P_a / (V_{lq} \rho_{lq} g)$ $P_a = N_p \rho_{lq} N_a^3 D_a^5$ $N_p = 1.2, \text{ (magnetic stirrer)}$ $\varphi_C \approx 1$

the liquid-solid mass transfer coefficient (on liquid side,  $k_s$ ) is made following the Table 1 rule. It is to notice that, for most of the organic drug molecules, the internal drug transport resistance is much higher than those in the external liquid film (that is  $D_{A,ef}/k_s \ll d_p$ ), so generally the external resistance to the mass transfer in the well-mixed bulk liquid is negligible.

The mass balance equations can be reduced by using the particle effectiveness factor and  $A_f^{sup}$  at interface instead of internal  $A_f^s$  (see details of Maria et al.<sup>26</sup>). By using a stiff integrator, with simultaneously fulfilment of flux equality at interface on every small time increment, the solution of the differential-algebraic model was obtained.

By solving the EKM for every defined delivery system, the dynamics of drug concentrations on the support, at the solid-liquid interface, and in the homogeneous (well-mixed) bulk-liquid is thus obtained. In contrast to the semi-empirical or overall diffusional models,<sup>13,25</sup> the EKM advantage is coming from its relative simplicity and capacity to predict the drug concentration evolution in every system compartment/phase for any initial condition. Besides, the model parameters are fully interpret-

able as physico-chemical significance, being independent on the drug initial load. The disadvantage relates to the steady experimental and computational efforts to identify and verify all model parameters. The EKM can be easily extended for approaching porous support particles of variate geometry (thin sheet, rectangular parallelepiped, cylinder of finite or infinite length, sphere), by simply adapting the particle effectiveness and external diffusivity evaluations for known initial and boundary conditions.<sup>27,28</sup>

## Factors influencing the drug release rate

In the pre-programmed drug delivery from inorganic porous supports, the release rate is adjusted by the system characteristics controlling the diffusion in the matrix, and eventually across the support membrane. The main factors influencing the process are the following:<sup>1-3,5,14,21,22,29</sup>

- crystalline / amorphous structure of the support;

- support texture (porosity, BET surface, pore volume, size and distribution, tortuosity);
- support size and shape (spherical, cylindrical tablet, thin film);
- the way to adsorb the drug on the support;
- size (cross diameter) and chemical structure (functional groups, heteroatoms) of the drug molecule;
- initial load / maximum uptake capacity of the drug on the (functionalized) support;
- type of functional groups of the support surface / linker and their interaction with the drug molecule;
- functionalization method (the solvent used, and coverage degree);
- drug diffusivity and solubility in the receptor body fluid;
- temperature, pH, and mixing degree of the bulk (external) receptor fluid;
- body fluid characteristics (chemical / enzymatic activators of the drug release).

From the large numbers of factors influencing the release rate, some are detailed below, to be further used in the model-based evaluations of the approached irinotecan-MCM-41 release system.

### Support particle size and shape

The literature data pointed out no significant differences in the drug release time between powder (with sub-millimetric or even 1–3 mm particle size) and disk (13 × 3 mm) supports of comparable porosity.<sup>23,29</sup> Even if the initial release rate for spherical particles is higher due to a higher surface area to volume ratio, no significant improvement in the release time is obtained for thin cylindrical tablets,<sup>29</sup> due to the very slow diffusion of the drug molecules in the porous support matrix. For instance, the effectiveness ( $\eta$ ) of a 0.2 mm MCM particle is 0.01 for irinotecan, and 0.23–0.50 for cephalosporins<sup>13,26</sup> (see evaluation formula of Table 1). The small molecular diffusivity of organic molecules leads to a small effective diffusivity  $D_{A,ef}$  of  $10^{-10} - 10^{-14} \text{ m}^2 \text{ s}^{-1}$ ,<sup>30</sup> while the external mass transfer coefficient  $k_s$  in the liquid film is much higher ( $10^{-5} - 10^{-8} \text{ m s}^{-1}$ ) depending on the mixing efficiency,<sup>31</sup> making the external diffusional resistance to be negligible.

### Average pore diameter

The pore size ( $d_{pore}$ ) is an important parameter in modulating the drug release time for the case of large drug molecules and/or small pore sizes. The internal diffusion of the drug is hindered by several factors, and the resulting effective diffusion coefficient

$D_{eff}$  includes (Table 1): the molecular diffusion (due to intermolecular collisions,  $D_A$ ); Knudsen diffusion (when pore diameters are of the same magnitude as the molecular free path); surface diffusion (neglected here); particle tortuosity ( $\tau_p$ ) (a measure of the tortuous path of drug transport in pores of geometry other than a straight cylinder); restricted diffusion of molecules of large cross-diameter ( $d_{A,t}$ ) related to the pore diameter (configurational diffusion,  $K_r$ ); drug re-adsorption on the pore walls during diffusion ( $K_p$ ).<sup>22</sup> As the pore size becomes more comparable to the drug molecule diameter, the release rate declines. For instance, Horcajada et al.<sup>14</sup> have found in the case of ibuprofen ( $d_{A,t} \approx 5 \text{ \AA}$ ) released from a modified MCM-41 support, an average release rate ratio of 200 / 100 / 60 / 50  $\text{mg g}^{-1} \text{ h}^{-1}$  for average pore size ( $\text{\AA}$ ) decreasing in the ratio of 36 / 33 / 27 / 25 respectively.

### Initial drug uptake on the support

Reported experiments confirmed that high initial drug loads on support (below the saturation level) increase the drug release rate ( $r_A$ ) due to a higher concentration gradient between solid surface ( $A_f^{sup}$ ) and liquid bulk ( $A^l$ , see Fig. 1). The release rate can be approximated by the Fickian relationship written for a spherical particle:<sup>13,26</sup>

$$r_A = -D_{A,ef} (\partial A_f^s / \partial x)_{sup} a_s \approx (\text{constant}) D_{A,ef} A_f^{sup}. \quad (1)$$

(where  $A_f^s$  = free-drug concentration at the contact surface between support and liquid; ‘sup’ = refers to the solid-liquid external interface;  $x$  = the diffusion direction in pores). For instance, Bajpai et al.<sup>3</sup> reported for the tetracycline release from a polymeric porous support an initial release rate ratio of 0.0065 / 0.004 / 0.002  $\text{mg min}^{-1}$  corresponding to initial load ratios of 66.6% / 56.6% / 43.3% respectively. Similar results have been presented by Maria et al.<sup>13</sup> when comparing the obtained  $r_{A,0}$  for various initial irinotecan loads on a MCM-41 support. It is to notice that the drug equilibrium levels on solid and in liquid depend on the initial and release conditions, liquid volume, and drug-support-liquid interactions.

### Silica support structure

Chemical composition and structure of the support is essential for its hydrophobic / hydrophilic character, and surface availability for linkers and drug molecules. For instance, MCM and SBA are very stable silica supports, of highly ordered structure, with a high density of silanol groups ( $2.5 - 5 \text{ nm}^{-2}$ )<sup>32</sup> easily to be functionalized.<sup>5</sup> MCM-41 includes hexagonal 1D channels of 20–50  $\text{\AA}$ , while

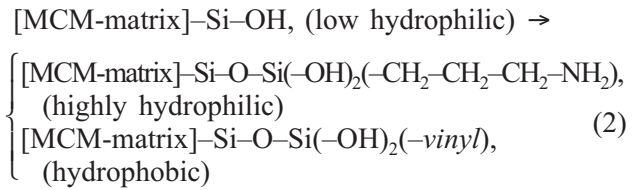
MCM-48 has a bicontinuous 3D structure and 20–50 Å pores. Similarly, SBA can present a variate matrix structure: 1D (SBA-15) or 2D (SBA-3) hexagonal channels of 20–50(100) Å size, body center arrangement of cages (SBA-16), or cubic structure with 20–40 Å pores (SBA-1). The support matrix characteristics can be modified by including various atoms in the silica crystal. For instance, Ji et al.<sup>19</sup> inserted Al in the silica MCM-41 matrix to increase its hydrophilicity, thus increasing the adsorption capacity of the support for polar molecules as the Si/Al ratio decrease (keeping similar BET area and pore sizes). Similarly, Li et al.<sup>16</sup> reported a slightly increase in the release rate of ibuprofen from a mesoporous silica SBA-15 support doped with Ca.

### Linker type

Another way to control the drug release rate is to modify the support surface properties by binding functional reactive or passive groups to accommodate guest molecules by physico-chemical interactions.<sup>1</sup> Such modifications affect the release rate and process specificity under certain release conditions, the release rate being dependent not only on the linker structure, but also on the surface functionalization method and degree.<sup>1,15,21</sup>

For instance, Maria et al.<sup>13</sup> modified the MCM-41 surface either by functionalization with

the hydrophilic APTES or with the hydrophobic VTES linker, following the grafting schema:



Compared to the basic support, the functionalized MCM-41 presents a BET area reduced from 1010 m<sup>2</sup> g<sup>-1</sup> to 730–850 m<sup>2</sup> g<sup>-1</sup>, a pore volume reduced from 1 cm<sup>3</sup> g<sup>-1</sup> to 0.52 cm<sup>3</sup> g<sup>-1</sup>, and a pore size reduced from 30 Å to 24–26 Å (Table 2). For the irinotecan release at 37 °C (buffer of pH = 7.4;  $d_p = 0.2$  mm particles), Maria et al.<sup>13</sup> derived several conclusions: I) the release is favoured by the hydrophilic surface, with an initial release rate in a ratio of 6.32 / 5.92 / 1 for MCM-41 / MCM-41-APTES / MCM-41-VTES supports respectively (rates calculated with eq. 1), even if the release time is practically the same (250–300 min); ii) the drug equilibrium levels on the support confirm this release tendency, being very low for MCM-41-APTES (0.01% of the initial load), comparatively to MCM-41-VTES (28.9% of the initial load; Table 2). These conclusions are also reflected by the EKM identified equilibrium constants, i.e.  $K > 1$  for MCM-APTES and  $K < 1$  for MCM-VTES.

Table 2 – Support characteristics, initial drug load, model parameters ( $k_1, K = k_2/k_1$ ), and equilibrium data for the irinotecan release from a MCM-41 silica support (functionalized with APTES or VTES). Experimental conditions correspond to: a synthetic intestinal body fluid (buffer solution of 39.5 mL NaOH 0.1 M, and 50.5 mL KH<sub>2</sub>PO<sub>4</sub> 0.1 M; pH = 7.4); 37°C; drug solubility ( $A_T^{\text{max}}$ ) of 13.3 g L<sup>-1</sup>; support maximum uptake capacity ( $A_b^{\text{s,max}}$ ) of 40%wt.; liquid volume of 90 mL; particle diameter  $d_p = 0.2$  mm; tortuosity  $\tau_p = 1.5\text{--}1.6$ ; magnetic stirrer speed  $N_a = 120\text{--}250$  rpm; solid volumetric fraction in the reactor  $\varepsilon_s = 4 \cdot 10^{-4}$  (L solid) (L liquid)<sup>-1</sup>;  $k_s a_s = 0.8\text{--}1.8 \cdot 10^{-6}$  (s<sup>-1</sup>) (after Maria et al.<sup>13</sup>; L-lq. denotes the liquid volume).

Parameter	Support-Linker-Drug		
	MCM41-Irinotecan	MCM41-APTES-Irinotecan	MCM41-VTES-Irinotecan
$S_{\text{BET}}$ (m <sup>2</sup> g <sup>-1</sup> )	1010	850	726
porosity $\varepsilon_p$	0.64	0.48	0.39
drug/pore size, $d_{A,t}/d_{\text{pore}}$ (Å/Å)	5 / 30	5/23.2	5/26
drug load / drug mass (%wt)/(mg)	35.8 / 14.8	34.9 / 15	36.3 / 15
linker (%wt) <sup>(*)</sup>	–	27.5	13.6
$k_1$ (min <sup>-1</sup> L g <sup>-1</sup> )	20.091	20.091	$1.268 \cdot 10^4$
$K = k_2/k_1$	0.241	1.752	$2.533 \cdot 10^{-2}$
$D_{ef}$ (m <sup>2</sup> s <sup>-1</sup> )	$2.4 \cdot 10^{-13}$	$4.4 \cdot 10^{-14}$	$3.8 \cdot 10^{-14}$
equilibrium ( $A_b^s$ ) <sub>eq</sub> (g L-lq <sup>-1</sup> )	0.0086 (5.2% $A_{b,0}^s$ )	0.0014 (0.01% $A_{b,0}^s$ )	0.0481 (28.9% $A_{b,0}^s$ )
equilibrium ( $A^l$ ) <sub>eq</sub> (g L-lq <sup>-1</sup> )	0.156	0.165	0.118

(\*) related to drug-free support.

The way to functionalize the support (by grafting, coating, or co-condensation reactions) is also responsible for the surface characteristics: homogeneous linker distribution, preservation of the matrix integrity, surface coverage degree.<sup>1</sup> For instance, Song et al.<sup>15</sup> revealed in the case of ibuprofen release (hydrophilic drug) from mesoporous silica SBA-15 functionalized with APTES, that post-synthesis reduces at half the release rate comparatively to the one-pot functionalized support case (even if the release time is practically the same, ca. 100 min). Zeng et al.<sup>11</sup> tested functionalization of MCM-41 with APTES by post-synthesis, co-condensation, and solvothermal process, and concluded in the case of aspirin release that co-condensation is the best method to get a better delivery rate (reduced with ca. 25%), by offering a mono-layer coverage of the support. Doadrio et al.<sup>21</sup> and Izquierdo-Barba et al.<sup>10</sup> revealed in the case of erythromycin release from SBA-15 (36 Å pores) or MCM-48 (57 Å pores) that an increase in the linker chain length (from C8: octyltrimethoxysilane to C18: octadecyltrimethoxysilane) and the use of acetonitrile solvent instead of toluene during surface grafting decrease at half the drug release rate.

#### Linker coverage degree and multi-functionalization

A homogeneous and highly covered surface with a mono-layer of linker molecules is the best option for increasing the matrix availability to the drug molecules without decreasing too much the pore size.<sup>1,11</sup> The drug uptake increases with the surface coverage up to a limit imposed by the functional group density resulted from the grafting reactions. For instance, in the MCM-41 case, the silanol group density on the silica surface is very high (2.5–5 Si-OH groups per nm<sup>2</sup>) compared to O-Si-O (0.22 groups per nm<sup>2</sup>),<sup>32</sup> the support displaying a high uptake capacity for many drugs. However, experiments indicate a maximum of 40–45%wt. linker content on the support for the employed grafting procedure.<sup>13</sup>

Incorporation of two or more functional groups in a “one-pot” synthesis is also possible, although the uniform disposal of functional groups and the coverage degree are not so controlled as by the grafting procedure. Literature includes various examples, for instance the simultaneous functionalization with APTES and phenyl or methyl groups.<sup>1</sup> The support bi-functionalization can be a worthy route to adjust the hydrophobic/hydrophilic character of the surface, thus adjusting the release rate and the process thermodynamics (partition constant). By using the proposed *in-silico* design approach, this idea will be further developed.

### **In-silico design of an irinotecan release system using functionalized MCM-41**

The chosen case study to test the *in-silico* design procedure is that of the irinotecan release from a functionalized MCM-41 silica support, under the nominal conditions specified in Table 2:<sup>13</sup> a synthetic intestinal fluid of pH = 7.4 at 37°C, by using spherical particles of  $d_p = 0.2$  mm diameter in an amount of 0.04% volumetric fraction in the reactor. The surface rate constants ( $k_1$ ,  $k_2$ ) presented in Table 2 have been estimated from separate experiments at different drug loads by using unfunctionalized support, or MCM-41 functionalized by grafting reactions with APTES (in absolute ethanol) or VTES (in n-heptane). The hydrochloride irinotecan molecule (an anticancer drug) includes both hydrophobic heterocycles (some with N), but also hydrophilic groups (C=O, C–OH, –O–).

Taking advantage of the very good EKM adequacy and robustness, an optimized irinotecan release system will be determined by simulations using MCM-41 support with hydrophilic APTES or hydrophobic VTES functionalizations. The advantage of such a rule is coming from the possibility to investigate a wider parametric space without requiring supplementary experiments, and from the possibility to easily correlate the apparent variables with the structural characteristics of the system.

#### Modulate the pore size

By support functionalization, the average pore size of the MCM-41 is reduced, and so is its porosity and BET area (Table 2). Depending on the functionalization degree, the pore size declines from 30 Å to ca. 20 Å, which is still much higher than the drug molecule diameter (5 Å). Simulation of irinotecan release from a MCM-41 support of various pore sizes (10–30 Å), by keeping the same initial drug load, clearly points out in Fig. 2 that pore size reduction leads to a significant decline of the release rate only when its size becomes comparable to that of the drug. Under these circumstances, a sharp decrease of the effective diffusivity  $D_{A,ef}$  is reported, leading to a smaller particle effectiveness ( $\eta$ ) and a slower release rate, though the process duration for reaching the quasi-equilibrium state is roughly the same. Such a result was proved experimentally for the functionalized MCM-41 case, resulting any reduction in the release rate for pores of 23–30 Å size.<sup>13</sup> Such an experimental and theoretical result does not confirm the conclusions of Horcajada et al.<sup>14</sup> for the case of ibuprofen ( $d_{A,t} \approx 5$  Å) release from modified MCM-41 supports, which reported a four times reduction in

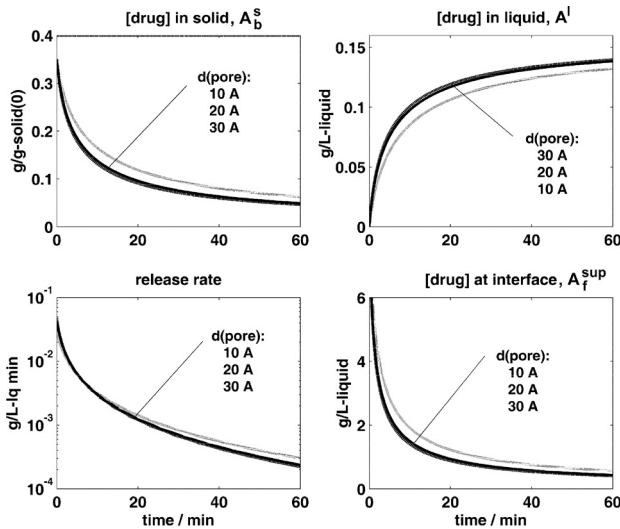


Fig. 2 – Influence of the pore size on the irinotecan release rate from a mezoporous support of MCM-41 (unfunctionalized) in the synthetic biological fluid, for pore diameters ( $d_{\text{pore}}$ ) of 10 Å, 20 Å, and 30 Å (initial drug load of  $A_{b,0}^s = 35\%$ wt.; nominal conditions of Table 2). Concentrations are referring to the liquid volume.

the release rate for a pore size reduction from 36 Å to 25 Å. In the last case, it is possible that other factors (e.g. the used surfactant) induce changes in the surface properties leading to the reported effect.

### Modulate the initial drug load

By applying a similar procedure, the effect of increasing the initial drug load of the irinotecan on the support ( $A_{b,0}^s \leq A_b^{s,\text{max}}$ ) is simulated for an unfunctionalized MCM-41 support under nominal conditions of Table 2. The results, plotted in Fig. 3, confirm the tendency reported in literature of a sharp increase in the initial release rate ( $r_{A,0}$ ) with the initial drug uptake due to a higher concentration gradient between solid surface and liquid bulk. However, the release time to reach the steady-state does not differ significantly for a wide range of initial loads of 0.05–0.35 g g<sup>-1</sup> (the maximum uptake capacity being 0.4 g g<sup>-1</sup>; other support characteristics are kept constant). A smoother release rate is obtained for a lower initial drug load on the support (0.05 g g<sup>-1</sup>). The results from employing functionalized MCM-41 (with APTES or VTES) are similar, even if the release rates are higher for the MCM-41-APTES due to the replacement of silanol (Si–OH) groups with Si–CH<sub>2</sub>–CH<sub>2</sub>–CH<sub>2</sub>–NH<sub>2</sub> groups leading to a more unstable linkage of the hydrochloride irinotecan, and to stronger interactions with the ionic fluid. Such predictions are in agreement with the experimental results of Maria et al.<sup>13</sup> when using unfunctionalized MCM-41 support with initial drug loads of 0.25 and 0.35 g g<sup>-1</sup>.

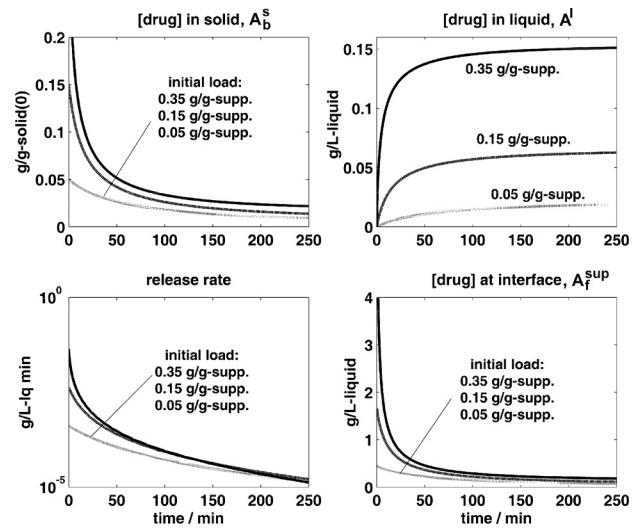


Fig. 3 – Influence of the initial drug load on the irinotecan release rate from a mezoporous support of MCM-41 (unfunctionalized) in the synthetic biological fluid, for initial drug load ( $A_{b,0}^s$ ) of 5%wt., 15%wt. and 35%wt. (pore diameters of 30 Å; nominal conditions of Table 2). Concentrations are referring to the liquid volume.

The increase of the initial drug load affects the equilibrium levels of the distributed drug between phases in contact. Model-based simulations for long release times indicate a significant increase of the irinotecan equilibrium concentrations in liquid and solid (Fig. 4). Experimental checks of the equilibrium levels have been reported for initial drug loads of 25% (unfunctionalized support) and 35% (both un-/functionalized supports).<sup>13</sup> As the release is favoured by the presence of APTES linker on MCM surface, the equilibrium value in the solid is much

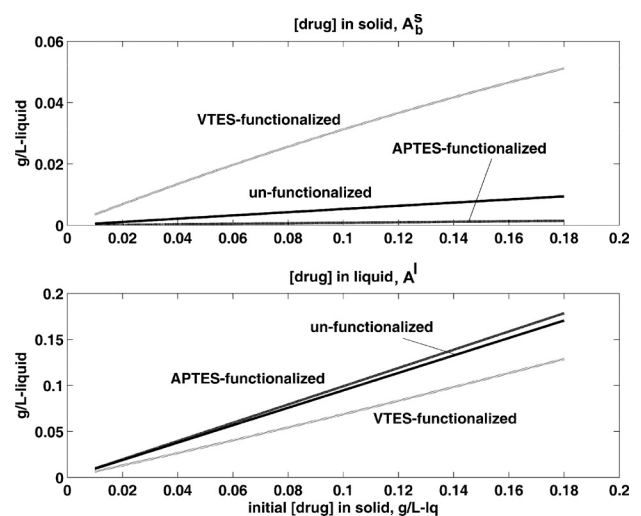


Fig. 4 – Influence of the initial drug load ( $A_{b,0}^s$ ) and of the MCM-41 support functionalization on the equilibrium concentrations of irinotecan in solid and liquid for the following supports: unfunctionalized MCM-41 (—), MCM-41-APTES (---), MCM-41-VTES (·) (nominal conditions of Table 2). Concentrations are referring to the liquid volume.



lower for the MCM-41-APTES than for the MCM-41-VTES support, and vice-versa in the bulk liquid. This release tendency is better quantified by the desorption-adsorption equilibrium constant  $K = k_2/k_1$ ; while for the hydrophilic MCM-41-APTES functionalization  $K$  constant is higher than unity (1.752 in Table 2), the release tendency is lower from the MCM-41 support ( $K = 0.241$ ), and much lower from the MCM-41-VTES support ( $K = 0.025$ ).

### Modulate the hydrophilic / hydrophobic balance through bi-functionalization

An interesting possibility of adjusting the release rate is to use a support functionalized with both hydrophilic and hydrophobic linkers. Thus, for a specific drug, the release rate can be easily modulated by changing the ratio of the two linkers on the support, by keeping unchanged the overall surface coverage. Bi-functionalization can be done by using the “one-pot” synthesis, or by mixing the powder support separately functionalized with each linker in the desired proportion.

To *in-silico* check this alternative, one considers the MCM-41 support with nominal characteristics of Table 2 (APTES column), but functionalized with both APTES and VTES, by keeping the overall coverage constant (27.5%wt). One assumes that the drug molecules preferentially bond to the free linker molecules of the support surface, while adsorption-desorption on other less active surface sites is of minor importance, being included in the apparent adsorption-desorption rate constants:

$$\begin{aligned} r_{ads} &= k_1 \theta^s A_f^s = k_1 (A_b^{s,max} - A_b^s) A_f^s \\ r_{des} &= k_2 \theta^l A_b^s = k_2 (A_f^{max} - A_f^s) A_b^s. \end{aligned} \quad (3)$$

For a bi-functionalized porous support with linkers L1 and L2, one considers a non-competitive drug linking process, the overall drug adsorption and desorption rates becoming:

$$\begin{aligned} r_{ads} &= (k_{1,L1} \theta_{L1}^s + k_{1,L2} \theta_{L2}^s) A_f^s \\ r_{des} &= (k_{2,L1} A_{b,L1}^s + k_{2,L2} A_{b,L2}^s) \theta^l. \end{aligned} \quad (4)$$

Consequently, for a constant surface coverage and denoting with  $g_{L1} = \theta_{L1}^s / \theta^s$  the gravimetric fraction of L1 active sites (L2 sites fraction being  $g_{L2} = 1 - g_{L1}$ ), the average adsorption and desorption rates can be formulated as follows:

$$r_{ads} = \bar{k}_1 \theta^s A_f^s; \quad r_{des} = \bar{k}_2 \theta^l A_b^s,$$

where:

$$\begin{aligned} \bar{k}_1 &= k_{1,L1} g_{L1} + k_{1,L2} g_{L2}; \\ \bar{k}_2 &= k_{2,L1} g_{L1} + k_{2,L2} g_{L2}; \quad \bar{K} = \bar{k}_2 / \bar{k}_1; \\ \theta^s &= \theta_{L1}^s + \theta_{L2}^s; \quad A_b^s = A_{b,L1}^s + A_{b,L2}^s; \\ K_{L1} &= k_{2,L1} / k_{1,L1}; \quad K_{L2} = k_{2,L2} / k_{1,L2}. \end{aligned} \quad (5)$$

(being assumed the equality of the ratios

$$A_{b,L1}^s / A_b^s = \theta_{L1}^s / \theta^s = g_{L1}$$

and

$$A_{b,L2}^s / A_b^s = \theta_{L2}^s / \theta^s = g_{L2}.$$

By applying this averaging procedure for the irinotecan adsorption-desorption on a bi-functionalized MCM-41-APTES-VTES support, one can simulate the drug release under the nominal conditions of Table 2 (centre column) and with known rate constants for every individual linker. By keeping the overall linker coverage of 27.5%wt., but varying the APTES linker fraction ( $g_{APTES}$ ) from 0 to 1 one obtains the release curves of Fig. 5, which lead to several conclusions.

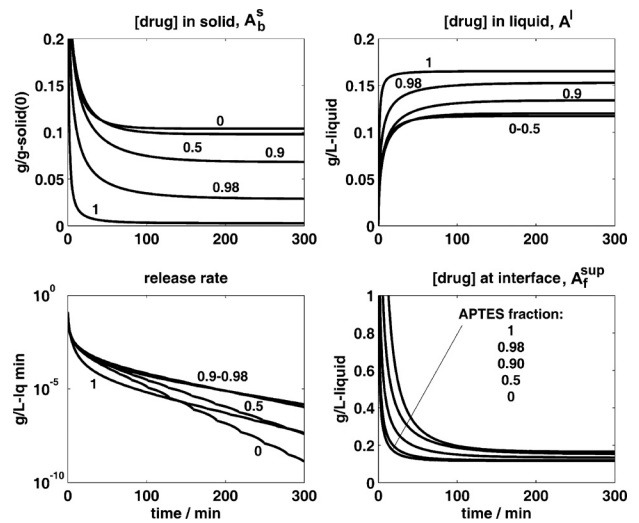


Fig. 5 – Simulation of the irinotecan release from a MCM-41 support, bi-functionalized with APTES and VTES, in the synthetic biological fluid, for initial drug load ( $A_{b,0}^s$ ) of 35%wt. The figured numbers on release curves denote the APTES wt. fraction on the covered surface with linkers (total linker coverage of 27.5%wt.; pore diameter  $d_{pore} = 24 \text{ \AA}$ ; porosity  $\varepsilon_p = 0.48$ ; particle diameter  $d_p = 0.2 \text{ mm}$ ; solid fraction in the reactor  $\varepsilon_s = 4 \cdot 10^{-4} \text{ L L}^{-1}$ ). Concentrations are referring to the liquid volume.

i) As expected, the irinotecan release rate from the bi-functionalized MCM-41 support is as high as the gravimetric fraction of APTES on the surface increases. Even more important, this dependence is strongly non-linear (roughly logarithmic): for up to

50% APTES the release curve is practically unchanged; in the range of 90–100% APTES the release curves change dramatically, in an accelerated way as  $g_{APTES}$  gets closer to 1. In absolute terms, for a 90%wt. APTES and 10%wt. VTES coverage, 80% of the irinotecan is released over 6 hrs. For comparison, over the same time interval, 72% of the drug is released for a 50%wt. coverage with APTES, but 92% of the drug is released for a 98%wt. coverage with APTES and 2% with VTES. In such a manner, the release time, rate, and the drug level in the liquid can be easily modulated by simply changing the ratio of hydrophilic / hydrophobic linkers on the support. It is also to observe that a smoother release rate can be achieved only for bi-functionalized supports with less than 50%wt. APTES coverage.

ii) An explanation of the logarithmic-like dependence of the drug release trajectory on the APTES fraction on the support can be offered by the pseudo-first order release rate for drug concentrations in the receptor fluid far from the saturation level. The process thermodynamics is also nonlinearly influenced by the  $g_{APTES}$  due to the hyperbolic dependence of the surface equilibrium constant:

$$\bar{K} = \frac{\bar{k}_2}{k_1} = \frac{k_{1,APTES} g_{APTES} + k_{1,VTES} (1 - g_{APTES})}{k_{2,APTES} g_{APTES} + k_{2,VTES} (1 - g_{APTES})} \quad (6)$$

It is to notice that the mono-layer functionalization degree on a silica support is however limited by the available density of silanol groups of the surface (e.g. 2.5–5 Si-OH groups per nm<sup>2</sup> for MCM),<sup>32</sup> and by the functionalization procedure.

Even if there is yet no experimental proof related to the predicted behaviour of the bi-functionalized MCM-41 support, the EKM simulations are expected to be well oriented, being based on consistent and robust parameters separately checked for the two types of functionalizations.

## Conclusions

A mechanism-based adequate kinetic model describing the drug release from a porous functionalized support can be a worthy instrument for predicting the process efficiency when using modified structures and operating conditions. Such *in-silico* evaluations can be realized if the model includes enough significant structural parameters of the system, eventually directing the experimental research toward finding an optimized drug-linker-support configuration that realizes the desired release rate. The EKM of Maria et al.<sup>13</sup> approached in this study can offer the possibility to evaluate the influence of some structural and operational process parameters

on the release efficiency and thermodynamic equilibrium, such as: pore size, support size and geometry, support modifications (e.g. via surface rate constants), porosity (pore volume), linker type, functionalization degree, linker ratio for a bi-functionalized support, drug molecule size and type, mixing conditions, temperature, pH.

The influence of some mentioned parameters are investigated in the case of irinotecan release from a mesoporous silica MCM-41 support functionalized with the hydrophobic APTES or hydrophobic VTES linkers, in a finite volume of synthetic body fluid at 37°C. Model based simulations results indicate some interesting conclusions concerning the release process: i) sub-millimetric particle size presents any significant influence on the release rate; ii) pore size exerts a significant influence only when it becomes comparable to the drug molecular diameter; iii) an increase of the initial drug load on the support leads to a sharp increase of the initial release rate but to a less smoother release; iv) the initial drug load strongly affects the equilibrium concentrations of the drug in support and liquid; v) the linker type strongly affects the release rate and equilibrium state, e.g. a high release tendency of irinotecan from MCM-41-APTES and much lower from MCM-41-VTES support; vi) changing the hydrophobic / hydrophilic linkers' ratio for a bi-functionalized MCM-41 support leads to a nonlinear variation of the release rate (and equilibrium state); vii) a smoother irinotecan release from a bi-functionalized support can be realized for a quasi-even surface coverage with the two linkers, at a moderate lower initial drug load on the carrier. Experimental checks of Maria et al.<sup>13,26</sup> validated some of the model predictions (i.e. influence of the pore size, initial drug load, and functionalization type on the process dynamics), some others remaining to be further confirmed.

Combinations of effects can be easily simulated with EKM, by simultaneously varying the process / support parameters, with also including factors not approached in this study (e.g. particle size and shape). The analysis can be easily extended for approaching other porous delivery systems of simple or multi-functionalization type, and for various support geometries (e.g. cylindrical tablets) without major changes in the model relationships.

## ACKNOWLEDGMENTS

*Financial support of the European Commission through the European Regional Development Fund and of the Romanian state budget, project POSCCE-O2.1.2-2009-2, ID 691, "New mesoporous aluminosilicate materials for controlled release of biologically-active substances" is gratefully acknowledged.*

**Symbols**

- $A_b^s$  – bound-drug on the support sites, g (L-lq)<sup>-1</sup>  
 $A_f^s$  – free-drug at the contact surface between support and liquid (in pores), g (L-lq)<sup>-1</sup>  
 $A_f^{sup}$  – free-drug at the solid-liquid external interface, g (L-lq)<sup>-1</sup>  
 $A^l$  – drug in the external solution (homogeneous bulk liquid), g (L-lq)<sup>-1</sup>  
 $A_b^{s,max}$  – active sites for drug adsorption on the support, g (L-lq)<sup>-1</sup>  
 $A_f^{max}$  – saturation level for the drug in liquid, g (L-lq)<sup>-1</sup>  
 $a_s$  – liquid-solid specific interfacial area, m<sup>-1</sup>  
 $D_a$  – stirrer diameter, m  
 $D_A$  – molecular diffusivity of A in the receptor fluid, m<sup>2</sup> s<sup>-1</sup>  
 $d_p$  – particle average diameter, m  
 $d_{A,t}$  – drug molecule width, m  
 $d_{pore}$  – pore average diameter, m  
 $g$  – gravimetric fraction; gravitational acceleration, m s<sup>-2</sup>  
 $K_p$  – partition coefficient for drug adsorption on the pore walls  
 $K_r$  – restriction coefficient for the hindered diffusion of large molecules vs. pore diameter  
 $k_s$  – liquid-solid mass transfer coefficient (on liquid side), m s<sup>-1</sup>  
 $k$  – rate constants, (L-lq) g<sup>-1</sup> s<sup>-1</sup>  
 $J_{diff}$  – diffusional rate of drug molecules in pores, g (L-lq)<sup>-1</sup> s<sup>-1</sup>  
 $M(t)$  – cumulative mass of drug released at time  $t$  in liquid  
 $M_\infty$  – cumulative mass of drug released at infinite time in liquid  
 $N_a$  – stirrer rotational speed, rpm  
 $N_p$  – dimensionless power number<sup>33</sup>  
 $n$  – Korsmeyer-Peppas model exponent  
 $P_a$  – power transmitted in the liquid by the magnetic stirrer<sup>34</sup>, W  
 $Re_L = (\sum_L d_p^4 \rho_L^3) / \mu_L^3$  – Reynolds number (liquid)  
 $r_A$  – adsorption / desorption rate of A species on the solid support, g (L-lq)<sup>-1</sup> s<sup>-1</sup>  
 $Sc_L = \mu_L / (\rho_L D_A)$  – Schmidt number (liquid)  
 $Sh = (k_s d_p) / D_A$  – Sherwood number  
 $t$  – time, s  
 $u_{s,L}$  – liquid superficial velocity (due to the mixing), m s<sup>-1</sup>  
 $V_{TP}$  – total volume of pores, m<sup>3</sup> g<sup>-1</sup>  
 $x$  – diffusion direction, m

**Greeks**

- $\epsilon_p$  – particle porosity  
 $\epsilon_s$  – volume fraction of particles in the bed, L solid (L-lq)<sup>-1</sup>  
 $\phi$  – Thiele modulus

- $\eta$  – effectiveness factor  
 $\theta^l = A_f^{max} - A_f^s$  – desorption potential due to the unsaturated liquid (with drug), g (L-lq)<sup>-1</sup>  
 $\theta^s = A_b^{s,max} - A_b^s$  – free sites on the support internal interface, g (L-lq)<sup>-1</sup>  
 $\mu$  – dynamic viscosity, N s m<sup>-2</sup>  
 $\rho$  – density, g L<sup>-1</sup>  
 $\Sigma_L$  – power dissipated per unit mass of liquid, m<sup>2</sup> s<sup>-3</sup>  
 $\tau_p$  – particle tortuosity  
 $\varphi_C$  – Carman shape factor<sup>28</sup>

**Index**

- ads – adsorption  
 b – bound drug  
 des – desorption  
 ef – effective  
 eql – equilibrium  
 f – free (unbound) drug  
 lq – liquid  
 o – initial  
 p – particle  
 s – referred to the solid phase, or to the interface, or to the steady-state

**Superscripts**

- l – referring to the liquid  
 max – maximum  
 sup – at the solid-liquid external interface  
 s – referring to the solid  
 – – average value

**Abbreviations**

- APTES – 3-aminopropyl triethoxysilane  
 AA – desorption activators in the receptor liquid  
 EKM – extended (compartmented) kinetic model  
 MIP – molecularly imprinted systems  
 VTES – triethoxyvinylsilane

**References**

1. Stein, A., Melde, B.J., Schroden, R.C., *Advanced Materials* **12** (2000) 1403.
2. Chien, Y.W., Lin, S., Drug delivery: Controlled release. In E. Mathiowitz (Ed.), *Encyclopedia of pharmaceutical technology*, Marcel Dekker Inc., New York, 2002. pp. 811–833.
3. Bajpai, A.K., Bajpai, J., Shukla, S., *Journal of Material Science: Materials in Medicine* **14** (2003) 347.
4. Winzenburg, G., Schmidt, C., Fuchs, S., Kissel, T., *Advanced Drug Delivery Reviews* **56** (2004) 1453.
5. Wang, S., *Microporous and Mesoporous Materials* **117** (2009) 1.
6. Maria, G., Luta, I., *Chemical Papers* **65** (2011) 542.

7. *Sellergren, B., Allender, C.J.*, Advanced Drug Delivery Reviews **57** (2005) 1733.
8. *Mayes, A.G., Whitcombe, M.J.*, Advanced Drug Delivery Reviews **57** (2005) 1742.
9. *Lin, C.X., Qiao, S.Z., Yu, C.Z., Ismadji, S., Lu, G.Q.*, Microporous and Mesoporous Materials **117** (2009) 213.
10. *Izquierdo-Barba, I., Martinez, A., Doadrio, A.L., Perez-Pariente, J., Vallet-Regi, M.*, European Journal of Pharmaceutical Sciences **26** (2005) 365.
11. *Zeng, W., Qian, X.F., Yin, J., Zhu, Z.K.*, Materials Chemistry and Physics **97** (2006) 437.
12. *Wu, Z., Jiang, Y., Kim, T., Lee, K.*, Journal of Controlled Release **119** (2007) 215.
13. *Maria, G., Berger, D., Nastase, S., Luta, I.*, Microporous and Mesoporous Materials **149** (2012) 25.
14. *Horcajada, P., Ramila, A., Perez-Pariente, J., Vallet-Regi, M.*, Microporous and Mesoporous Materials **68** (2004) 105.
15. *Song, S.W., Hidajat, K., Kawi, S.*, Langmuir **21** (2005) 9568.
16. *Li, X., Zhang, L., Dong, X., Liang, J., Shi, J.*, Microporous and Mesoporous Materials **102** (2007) 151.
17. *Tang, Q., Xu, Y., Wu, D., Sun, Y., Wang, J., Xu, J., Deng, F.*, Journal of Controlled Release **114** (2006) 41.
18. *He, Q., Shi, J., Chen, F., Zhu, M., Zhang, L.*, Biomaterials **31** (2010) 3335.
19. *Ji, L., Katiyar, A., Pinto, N.G., Jaroniec, M., Smirniotis, P.G.*, Microporous and Mesoporous Materials **75** (2004) 221.
20. *Vergnaud, J.M., Rosca, I.D.*, Assessing bioavailability of drug delivery systems, CRC Taylor & Francis, Boca Raton, 2005.
21. *Doadrio, J.C., Sousa, E.M.B., Izquierdo-Barba, I., Doadrio, A.L., Perez-Pariente, J., Vallet-Regi, M.*, Journal of Materials Chemistry **16** (2006) 462.
22. *Narasimhan, B., Mallapragada, S.K., Peppas, N.A.*, Release kinetics, data interpretation. In: *E. Mathiowitz* (Ed.), Encyclopedia of controlled drug delivery, Wiley, New York, 1999. pp. 921–935.
23. *Doadrio, A.L., Sousa, E.M.B., Doadrio, J.C., Perez-Pariente, J., Izquierdo-Barba, I., Vallet-Regi, M.*, Journal of Controlled Release **97** (2004) 125.
24. *Ferrero, C., Massuelle, D., Doelker, E.*, Journal of Controlled Release **141** (2010) 223.
25. *Vergnaud, J.M.*, Controlled drug release of oral dosage forms, Ellis Horwood Publ., New York, 1993.
26. *Maria, G., Stoica, A.I., Luta, I., Stirbet, D., Radu, G.L.*, Microporous and Mesoporous Materials **162** (2012) 80.
27. *Doraiswamy, L.K., Sharma, M.M.*, Heterogeneous reactions: Analysis, examples, and reactor design, Wiley, New York, 1984, vol. 1–2.
28. *Trambouze, P., Van Landeghem, H., Wauquier, J.P.*, Chemical reactors: Design, engineering, operation, Edition Technip, Paris, 1988.
29. *Andersson, J., Rosenholm, J., Areva, S., Linden, M.*, Chemistry of Materials **16** (2004) 4160.
30. *Cybulski, A., Moulijn, J.A., Stankiewicz, A.*, Novel concepts in catalysis and chemical reactors, Wiley, New York, 2010.
31. *Deckwer, W.D., Becker, F.U., Ledakowicz, S., Wagner-Doebler, I.*, Environmental Science and Technology **38** (2004) 1858.
32. *Shenderovich, I.G., Buntkowsky, G., Schreiber, A., Gedat, E., Sharif, S., Albrecht, J., Golubev, N.S., Findenegg, G.H., Limbach, H.H.*, Journal of Physical Chemistry B **107** (2003) 11924.
33. *Perry, R.H., Green, D.W., Maloney, J.O.*, Perry's chemical engineers' handbook, McGraw-Hill, New York, 1997.
34. *Paul, E.L., Atiemo-Obeng, V.A., Kresta, S.M.*, Handbook of industrial mixing: Science and practice, Wiley, New York, 2004.
35. *Doran, P.M.*, Bioprocess engineering principles, Elsevier, Amsterdam, 1995.
36. *Shen, L., Chen, Z.*, Chemical Engineering Science **62** (2007) 3748.